IMPERIAL

SUMMER RESEARCH PROJECT REPORT

IMPERIAL COLLEGE LONDON

DEPARTMENT OF CHEMISTRY

Mixed feedstock screening of IonoSolv fractionation

Author:
Rashed Mahmoud Jastaniah

Supervisors:
Suhaib Nisar
Jason P. Hallett
Agnieszka Brandt-Talbot

Date: November 14, 2025

Unpublished research report submitted for Laidlaw Scholarship for Leadership and Research programme requirements

Contents

1 Abstract

Efficient lignocellulosic biomass fractionation is critical for a sustainable bioeconomy. The IonoSolv process, using protic ionic liquids like triethylammonium hydrogensulfate ($[TEA][HSO_4]$), is a promising pretreatment technology. However, while single feedstock processing is well-documented, the co-processing of mixed feedstocks, which is vital for biorefinery flexibility, remains largely unexplored. This study investigates the IonoSolv pretreatment of mixed *Miscanthus gianteus* (grass) and *Pinus sylvestris* (softwood) feedstocks at various mixing ratios and processing conditions. Fractionation performance was quantified using near-infrared (NIR) spectroscopy, and the extracted lignin structure was analysed by 2D HSQC NMR. We found that glucan recovery and hemicellulose removal exhibited a predictable,additive effect, closely matching a weighted average of the single-feedstock controls. In contrast, delignification was non-additive and optimized in 1:1 (w/w) blends, likely due to balanced mass transfer and ionic liquid solvating capacity. Mechanistically, HSQC analysis revealed no evidence of chemical cross-condensation between the two lignin populations. Critically, syringyl (S) units, characteristic of *Miscanthus*, were completely absent from the precipitated lignin of mixed systems, indicating that co-processing is governed by sequential extraction kinetics (driven by different lignin glass transition temperatures) and selective precipitation of G-rich pine lignin. These findings demonstrate the technical feasibility of co-processing and open new strategies for staged lignin fractionation in flexible biorefineries.

2 Introduction and background

The transition towards a sustainable bioeconomy requires the efficient conversion of lignocellulosic biomass into value-added chemicals, materials, and fuels [1]. Lignocellulosic biomass, comprising cellulose, hemicellulose, and lignin, represents an abundant renewable feedstock that does not compete with food production [2]. However, the recalcitrant nature of lignocellulosic biomass, particularly the complex lignin-carbohydrate matrix, necessitates effective pretreatment strategies to enable subsequent enzymatic hydrolysis and fermentation processes.

Ionic liquid (IL) pretreatment has emerged as a promising technology for biomass fractionation, offering advantages including low volatility, thermal stability, and the ability to dissolve both lignin and polysaccharides under mild conditions [3]. Among various ionic liquids, protic ionic liquids (PIL) containing the hydrogensulfate (HSO_4^-) anion have demonstrated particular promise due to their low cost, ease of synthesis, and effective delignification capabilities [4]. The IonoSolv process, employing triethylammonium hydrogensulfate ($[TEA][HSO_4]$), has shown exceptional performance in fractionating various biomass feedstocks, achieving high cellulose recovery while selectively extracting lignin and hemicellulose [5].

Previous studies have extensively characterized the IonoSolv pretreatment of individual feedstocks. For grass feedstocks such as *Miscanthus giganteus*, rapid and effective delignification has been demonstrated at temperatures of $120 - 180°C$, with the process preserving cellulose crystallinity while extracting syringyl-guaiacyl-

hydroxyphenyl (S-G-H) lignin [6]. The extracted *Miscanthus* lignin exhibits relatively low molecular weight and contains significant β–O–4 linkages that can be valorized through depolymerisation [7]. In contrast, softwood feedstocks like *Pinus sylvestris* present greater challenges due to their higher lignin content and guaiacyl-only lignin structure, which exhibits greater recalcitrance towards pretreatment [8]. The glass transition temperature (T_g) differences between softwood lignin ($170 - 240°C$) and grass lignin ($130 - 150°C$) significantly influence extraction kinetics and process optimization [9].
While single feedstock processing has been well-studied, the co-processing of mixed feedstocks remains largely unexplored despite its potential advantages for biorefinery operations. Mixed feedstock processing could offer benefits including improved feedstock flexibility, reduced seasonal variability, and potentially synergistic effects during pretreatment. The interaction between different lignin types (e.g., S-G-H grass vs. G-only softwood) during ionic liquid pretreatment may influence extraction efficiency, lignin precipitation behaviour, and product quality. Understanding these interactions is crucial for developing integrated biorefineries capable of processing diverse feedstock streams.
This study investigates the IonoSolv pretreatment of mixed *Miscanthus*-pine feedstock systems to elucidate potential synergistic or antagonistic effects during co-processing. By systematically varying mixing ratios and pretreatment conditions, we aim to understand the fundamental interactions between grass and softwood lignin populations during ionic liquid fractionation. Using compositional analysis through near-infrared (NIR) spectroscopy and detailed structural characterization by 2D HSQC NMR, we assess pretreatment performance and probe the chemical mechanisms governing mixed-feedstock delignification to establish processing strategies for integrated biorefinery operations.

3 Materials and Methods

Starting materials for ionic liquid synthesis were purchased from Sigma Aldrich and used as received, unless stated otherwise. HSQC spectra were recorded on a Bruker 800 MHz spectrometer. Chemical shifts (δ) are reported in ppm. The DMSO–d_6 solvent signal was at 2.500 (^{1}H dimension) and 39.520 (^{13}C dimension). The Karl Fischer titrator used was a Mettler-Toledo V20 Volumetric Titrator. Acid-base ratio was determined with a Mettler Toledo G20S compact titrator. Near-Infrared (NIR) spectra were recorded on an Agilent Cary 500 UV-Vis-NIR spectrometer with a DRA-2500 internal diffuse reflectance accessory.

3.1 Materials

3.1.1 Biomass Feedstocks

Lignocellulosic biomass (*Miscanthus* (*Miscanthus giganteus*) and pine (*Pinus sylvestris*) were air-dried, milled to the desired specifications (Table 1) and stored at room temperature in sealed containers away from light. Biomass mixtures were prepared

gravimetrically: 1:1, 1:2, and 2:1 Pine:*Miscanthus* (w/w). Single feedstock controls were prepared identically. Composition of untreated biomass by NREL protocol [10]: *Miscanthus* (50.1% cellulose, 22.4% hemicellulose, 26.8% lignin, 0.7% ash)[6], Pine (43.4% cellulose, 19.1% hemicellulose, 32.2% lignin, 0.8 % ash)[8].

Table 1: Specifications of raw biomass

Biomass	Type	Particle size (μm)
Miscanthus	Perennial grass	$180 \leq x \leq 850$
Pine	Softwood	$180 \leq x \leq 850$

3.1.2 Ionic Liquid synthesis

Starting materials for ionic liquid synthesis were purchased from Sigma Aldrich and used as received, unless stated otherwise. Triethylammonium hydrogensulphate ([TEA][HSO_4]) was synthesised by dropwise addition of 5M sulphuric acid (1 equiv) to triethylamine (1 equiv) cooled in an ice bath while under continous stirring. Reaction vessel is sealed and left to stir overnight. The ionic liquid recovered is a clear, colourless, viscous and hygroscopic liquid. Titration against NaOH was conducted to determine and adjust the acid-base ratio whereas Karl Fischer titration was used to aid further adjustment to reach the optimum 20wt% water content [11, 5].

3.2 Fractionation of lignocellulosic biomass

Pretreatments were carried out according to a standard operating procedure from our laboratory [5]. A biomass to solvent ratio of 1:10 gg^{-1} was used with 80wt% [TEA][HSO_4] and 20wt% water as the solvent. The precipitated lignin fraction was further freeze-dried to aid in cellulose yield calculation and understanding delignification performance. A detailed description of the procedure can be found in the ESI†. Pretreatment conditions are highlighted in Table 2.

Table 2: Fractionation conditions

Reference	Temperature (°C)	Duration (min)	Acid-Base ratio
T1	150	90	0.993
T2	170	60	0.993
T3	160	60	1.005
T4	160	60	0.993
T5	170	60	1.005
T6	170	120	0.993
T7	170	120	1.005

3.3 Analytical methods

3.3.1 Near-infrared (NIR) spectroscopy

NIR spectra were recorded on an Agilent Cary 5000 UV-Vis-NIR spectrometer following the protocol in Nisar *et al.* [12] Each sample was packed into a solid powder cell, with reflectance (%) measurements collected at 4 nm intervals. Four scans were taken for each sample with the powder cell rotated 90° between scans to minimise scattering effects. Spectrometer settings are detailed in the ESI†.
Spectra were processed to determine compositional analysis through an open-source Partial Least Squares (PLS) model [12].

3.3.2 HSQC NMR spectroscopy

ca. 12 mg of lignin was dissolved in DMSO–d_6 (900 mg, 0.76 mL) solvent and the solution was transferred to an NMR tube. HSQC NMRs were recorded on a Bruker 800 MHz spectrometer (pulse sequence hsqcetgpsi2, spectral width of 10.0 ppm in F2 (^{1}H) with 1024 data points and approximately 165 ppm in F1 (^{13}C) with 256 data points, 8 scans and 1.5 s interscan delay).
Spectra were analysed using MestReNova (Version 16.0.0, Mestrelab Research 2025). All spectra were referenced to the DMSO peak at 2.500 ppm (1H) and 39.520 ppm (13C). The HSQC spectra were used to estimate relative the amounts of aromatic rings (guaiacyl, syringyl, p-hydroxyphenyl and p-coumaric acid) in the lignin by volume integration of relevant peaks using the MestReNova software noting that the symmetric S, H and PCA rings contribute two C–H pairs per peak. All spectra can be found in ESI†.

3.4 Data analysis

Single measurements reported for investigation. Full statistical validation (n ≥ 3) identified as a priority for future work.

3.4.1 Severity Factor

Pretreatment conditions in lignocellulosic biorefinery studies are defined by the severity factor relationship (Eqn 1) first proposed by Chornet and Overend [13] and applied to IonoSolv by Malaret et al. [14] where R_0 is the severity factor, T is the temperature of the reaction medium in $°C$, T_{ref} is a reference temperature, t is time in minutes and ω is a parameter expressing the effects of temperature in the specific reaction considered. Typical values used for T_{ref} and ω are 100 $°C$ and 14.75, respectively [15] which are also used in this study.
Eqn 1's relationship assumes a constant acidity [14, 13] which doesn't reflect the significant impact of the ionic liquid's acid-base ratio on pretreatment conditions. Therefore, a revised version of Eqn 1 is proposed to describe severity in Eqn 2 where $H_\propto$ is the acid-base ratio and γ is a statistically-optimised coefficient determined to be 20 for this study's dataset; optimisation methodology is further explored in the

ESI. The severity factor is subsequently normalised using Eqn 3 for easier graphical visualisation.
We acknowledge that a more robust severity factor equation was previously developed [16] to incorporate Hammett acidity (H_0) which quantifies the acidity of non-aqueous systems such as ionic liquids, however, Eqn 2 compensates for the lack of definitive measurements of ionic liquid acidity during the study.

$$R_0 = t \cdot \exp\left(\frac{T - T_{ref}}{\omega}\right) \tag{1}$$

$$R_{0\gamma} = t \cdot \exp\left(\frac{T - T_{ref}}{\omega} + \gamma(H_\propto - 1)\right) \tag{2}$$

$$R_{0,\text{scaled}} = \frac{R_{0\gamma} - R_{0\gamma,\text{min}}}{R_{0\gamma,\text{max}} - R_{0\gamma,\text{min}}} \tag{3}$$

Table 3: Corresponding $R_{0,\text{ scaled}}$ to fractionation conditions investigated

Temperature (°C)	**Duration (min)**	**Acid-Base Ratio**	$R_{0\gamma}$	$R_{\mathbf{0,scaled}}$
150	90	0.993	2321	0.0000
160	60	0.993	3048	0.0562
160	60	1.005	3874	0.1200
170	60	0.993	6004	0.2845
170	60	1.005	7632	0.4103
170	120	0.993	12007	0.7484
170	120	1.005	15264	1.0000

3.4.2 Compositional Analysis

An NIR-based PLS compositional analysis model [12] was used after validating accuracy for the mixed feedstocks against standard NREL protocol [10]. Model outputs are used to calculate key performance metrics: Glucan recovery, Hemicellulose removal, Delignification shown in Equations (4)–(6).

$$\text{Glucan Recovery} = \frac{\text{Glucan}_{NIR} \times \text{Yield}_{pulp}}{\text{Glucan}_{untreated}} \tag{4}$$

$$\text{Hem. removal} = 1 - \frac{\text{Hem.}_{NIR} \times \text{Yield}_{pulp}}{\text{Hem.}_{untreated}} \tag{5}$$

$$\text{Delign.} = 1 - \frac{\text{Lignin}_{NIR} \times \text{Yield}_{pulp}}{\text{Lignin}_{untreated}} \tag{6}$$

4 Results and Discussion

4.1 Physical appearance

Cellulose colouration was consistent for both single and mixed feedstocks, where light and dark shades commonly represent under and over-treated samples, respectively. This could be a result of re-precipitated pseudo-lignin and humins [17] ergo a consequence of severity.

Morphology of the cellulose pulps observed with the naked eye were inconsistent for all samples ranging between being coarse-fibrous and being lumpy-compacted or even both. Highly over-treated samples begin to char and become ash-like. It is important to note that the retention of cellulose crystallinity, in the native form of cellulose-I, is a characteristic feature of IonoSolv pretreatment [18]. Therefore, cellulose lattice structure could be reasonably disregarded as a factor in the observed effects. This inconsistency in texture is more likely attributed to physical handling as well as the centrifuge-dependent washing method in the experimental protocol [19].

Other reported effects of IonoSolv pretreatment include an increase in surface area and decrease in pore size, which is partially a consequence of the expansion of the interchain cellulose hydrogen bonding [17] shown in Fig 1A.

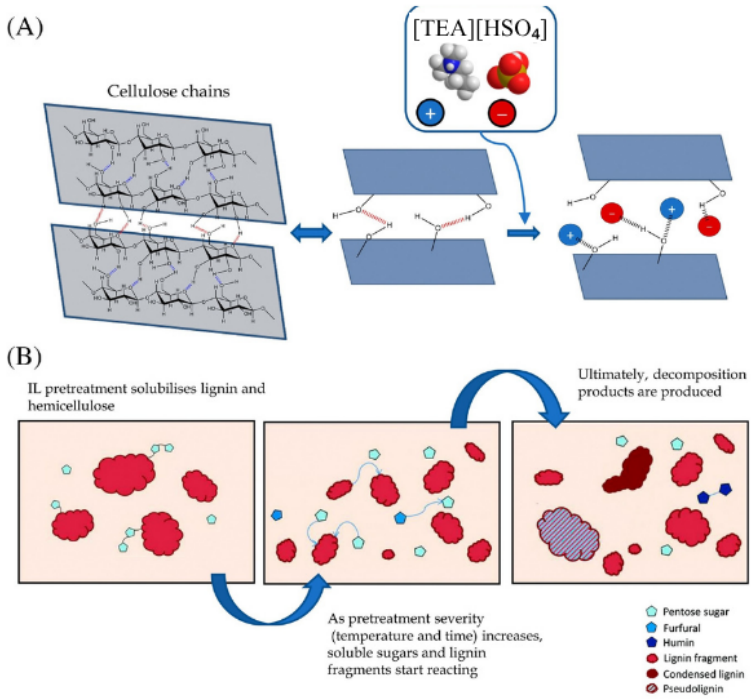

Figure 1: The effect of protic ionic liquid (PIL) pretreatment on lignocellulosic biomass. Adapted from ref.[17] with permission from Elsevier, Copyright 2022.

4.2 Solid loading

The solid loading ratio limits mass transfer when the biomass isn't fully submerged in the ionic liquid [19, 8]. This issue was evident with pine, which formed compacted lumps exposing a dry core during vortex shaking with the ionic liquid before pretreatment, indicating incomplete contact with the ionic liquid despite long soaking times. In contrast, *Miscanthus* was fully submerged. This suggests that 1:5 gg^{-1} solid loading is likely too high for pine, causing the ionic liquid to stop functioning as a solvent and thereby limiting mass transfer [19].

Consequently, the variability in bulk density between pine (138–264 kg m^{-3})[20] and *Miscanthus* ($\sim$ 200–300 kg m^{-3})[21] made it difficult to achieve a fully homogenous mixed system with the already viscous $[TEA][HSO_4]$ for pretreatment. It is unclear the extent of this effect on observing cross-feedstock interactions.

4.3 Compositional Analysis

Glucan recovery, hemicellulose removal and delignification are the primary metrics for assessing IonoSolv fractionation performance [2] as they directly measure how well the process achieves its goal: lignin and hemicellulose removal while preserving cellulose (glucan) stability for downstream processing [22].
An additive interaction in mixed feedstock systems implies no impact on fractionation performance in mixed feedstock systems. Therefore, single feedstock pretreatments were taken as controls to elucidate the nature of interaction in mixed feedstock systems, where a purely additive effect was defined as a simple weighted average of the single feedstock values at each pretreatment condition (Equation 7). Since only single measurements were collected for each condition and mixing ratio, deviations of ±5% from the additive prediction were disregarded: they are likely a consequence of statistical standard deviation rather than a physical observation. Most favourable yields were obtained at $3000 < R_{0\gamma} < 6000$; lower $R_{0\gamma} < 3000$ result in incomplete pretreatment whereas high $R_{0\gamma} > 6000$ cause charring and degradation of products.

$$\text{Performance}_{Theoretical} = (\text{Misc. ratio} \times \text{Metric}_{Misc.}) + (\text{Pine ratio} \times \text{Metric}_{Pine}) \quad (7)$$

4.3.1 Glucan recovery and hemicellulose removal

Mixed feedstock systems, irrespective of mixing ratio, showed high glucan recovery and hemicellulose removal closely aligned with single feedstock performance and predictions of an additive effect (Fig. 2, 3). This is strongly suggestive of an additive effect in mixed feedstock blends. Overall, hemicellulose removal and glucan recovery matches previous findings on $[TEA][HSO_4]$ performance with *Miscanthus* and pine feedstocks[6, 8].

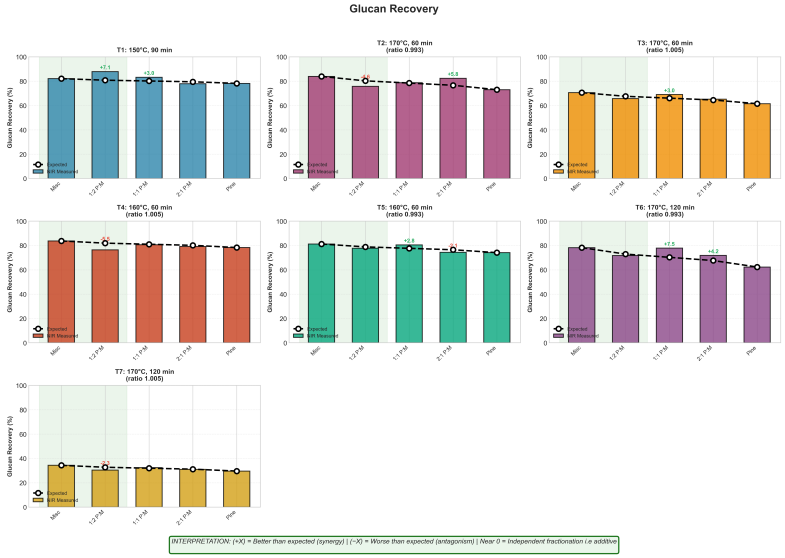

Figure 2: Glucan recovery at various mixing ratios. Expected values are mathematical weighted averages and the dotted lines is a visual aid and isn't suggestive of trends. Green-shaded region highlights *Miscanthus*-rich ratios

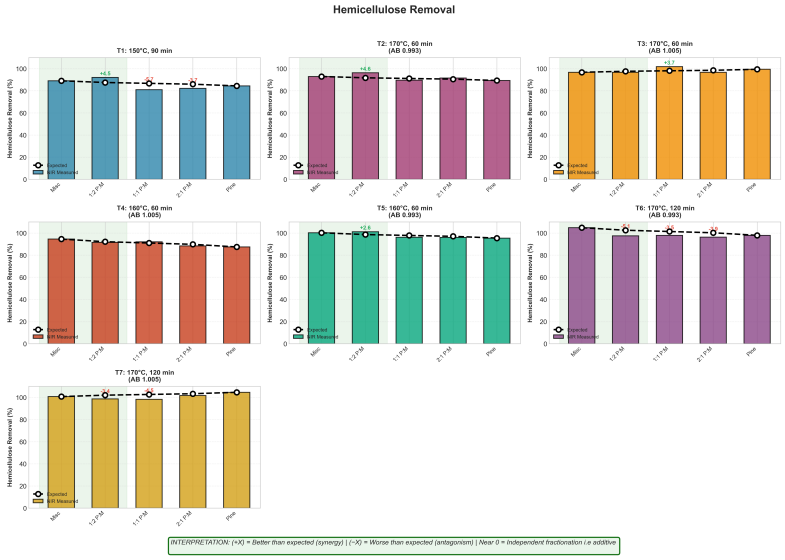

Figure 3: Hemicellulose removal at at various mixing ratios. Expected values are mathematical weighted averages and the dotted lines is a visual aid and isn't suggestive of trends. Green-shaded region highlights *Miscanthus*-rich ratios

4.3.2 Delignification

Gschwend et al. [8] highlights that pine lignins are inherently more recalcitrant towards pretreatments compared to grasses due to the higher lignin content [23] consisting largely (95%) of guaicyl (G) units[9]. Therefore, higher pretreatment temperatures were performed in this study to prompt softwood pretreatment as it is theorised that lignin extraction is facilitated above the glass transition temperature (T_g) [8, 24].

While glucan recovery and hemicellulose removal were strongly suggestive of the mixed feedstock systems being additive, delignification (Fig. 4) shows different deviations suggesting a reinterpretation of mixed feedstock behaviour. Indeed, it was expected that *Miscanthus*-rich blends would have the highest delignification as a direct consequence of pseudo-lignin formation due to the higher reactivity of *Miscanthus* [6] and a lower T_g (130 – 150 °C) [24] compared to pine (T_g: 170– 240 °C [25]). However, regardless of severity, 1:1 blends generally showed the highest delignification compared to other mixing ratios.
The observed effect is likely caused by sequential extraction kinetics as *Miscanthus* lignin extracts more readily and rapidly than pine lignin [6]. Furthermore, heating during pretreatment is non-isothermal and non-instantaneous, therefore, the delignification threshold for *Miscanthus* is achieved thereby saturating the ionic liquid before pine lignin extraction. Additionally, this kinetic effect suggests that pine surface may also be coated with re-precipitated *Miscanthus* lignin [19] which subsequently hinders pine delignification. The 1:1 mixing ratio may also provide better spatial distribution where *Miscanthus* particles interspersed within pine prevent large zones of pure grass material that could form localized high lignin concentration microenvironments. Thus it is proposed that the optimal mixing ratio is achieved in a 1:1 *Miscanthus*/pine blends (w/w) where the IL solvating capacity is maintained sufficiently for pine lignin extraction.

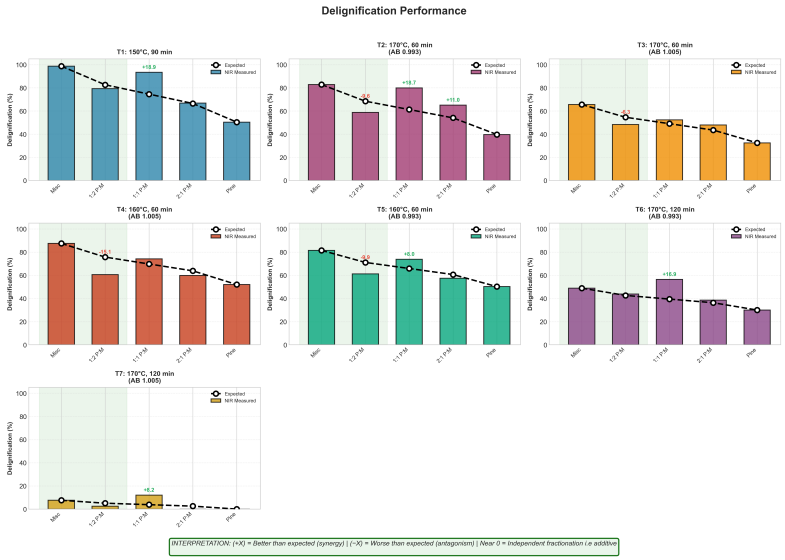

Figure 4: Delignification performance at various mixing ratios. Expected values are mathematical weighted averages and the dotted lines is a visual aid and isn't suggestive of trends. Green shaded region highlights *Miscanthus*-rich ratios

4.4 HSQC spectroscopy

To comprehensively screen for the effects of IonoSolv fractionation with mixed-feedstock blends, freeze-dried lignin from high severity pretreatments ($R_{0\gamma} > 5000$) were investigated. ^{1}H –^{13} C HSQC experiments were conducted as they give more

detailed information than compositional analysis on chemical interactions occurring during pretreatment [26, 7].
Native *Miscanthus* lignin mainly contains syringyl (S) and guaiacyl (G) phenolic subunits with smaller amounts of *p*-hydroxyphenyl (H), *p*-coumaric acid (PCA) and ferulic acid (FA) [7] whereas pine mostly contains G with small quantities of H subunits [27, 28]; relevant subunits and substructures are depicted in Fig. 5.

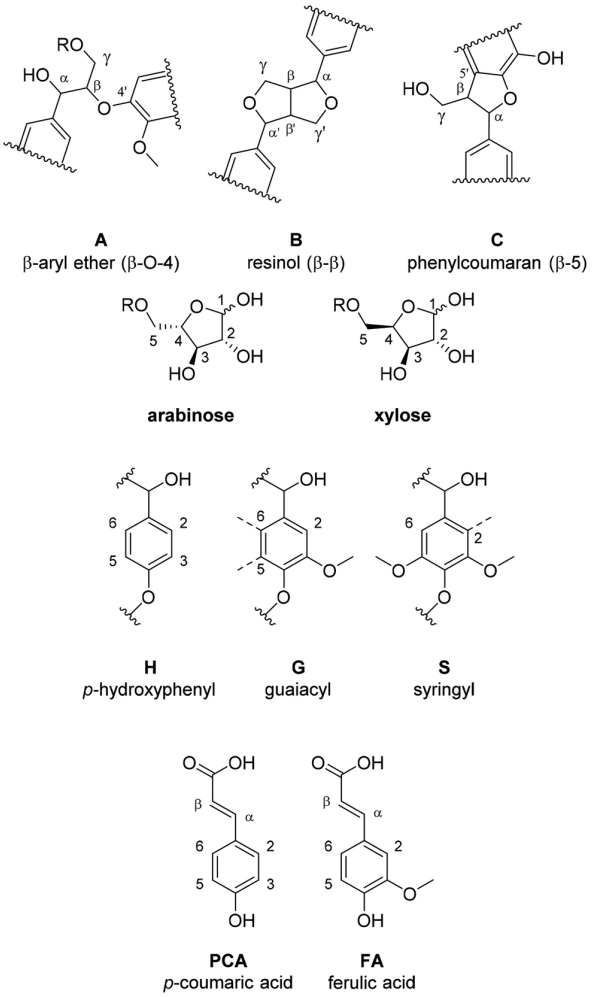

Figure 5: Lignin subunits and substructures

Cross-peak assignments were made with cell wall model compounds in an NMR database alongside previously reported HSQC spectra for lignin from IonoSolv pretreatments [7, 29, 30, 31, 32, 33, 34]; full annotated spectra and cross-peak assignments found in ESI. Lignin subunit composition was estimated semi-quantitatively by volume integration of $S_{2,6}$, G_2 and $H_{2,6}$ peaks [7] (see Table 4).

Single feedstock spectra were taken as controls to elucidate mixed feedstock behaviour in identical conditions. Reported *Miscanthus* lignin compositions in literature is 52% G, 44% S and 4% H[35], however, measured spectra show *Miscanthus* to have significantly higher H units which could be attributed to the limitation of optimising the HSQC pulse sequence for high resolution and signal strength instead

Table 4: Semi-quantitative estimate of lignin subunit composition after IonoSolv fractionation

Sample	G (%)	S (%)	H (%)	S/G	H/G	S:G:H
T3: 170°C, 60 min, 1.005 acid-base ratio						
Miscanthus	19.6	33.3	47.1	1.70	2.40	33:20:47
Pine	100	0	0	0	0	0:100:0
Mixed	78.9	0	21.1	0	0.27	0:79:21
T6: 170°C, 120 min, 0.993 acid-base ratio						
Miscanthus	46.7	28.1	25.2	0.60	0.54	28:47:25
Mixed	74.3	0	25.7	0	0.35	0:74:26
T7: 170°C, 120 min, 1.005 acid-base ratio						
Miscanthus	58.0	24.8	17.2	0.43	0.30	25:58:17
Pine	100	0	0	0	0	0:100:0
Mixed	100	0	0	0	0	0:100:0

of quantification [7].

HSQC spectra of pine/*Miscanthus* mixed blends further build on findings reported in compositional analysis. Mixed-feedstock spectra showed $S_{2,6}$ peaks fully absent while PCA_β/FA_β peaks (δ_H/δ_C 7.15/113.6 ppm), diagnostic grass indicators [30], were consistently preserved. This disappearance likely results from preferential extraction and degradation kinetics rather than cross-feedstock chemical reactions.

S-rich *Miscanthus* lignin extracts rapidly during initial heating phases in pretreatment. At 170 $°C$, conditions are well above *Miscanthus* lignin's T_g[24] but at the lower bound for pine lignin (T_g: $170 - 240°C$)[25], therefore, S units are extensively degraded and condensed which is supported with the fact that 42.4–83% of S units were condensed or oxidised† . However, syringyl aromatic signals are clearly present in pure *Miscanthus* controls ($S_{2,6}$ δ_H/δ_C 6.97/103.95 ppm) which indicates that mixed samples undergo selective lignin precipitation rather than complete degradation. Persistence of strong methoxyl signals (δ_H/δ_C 3.75-3.81/55.43 ppm) across all samples with comparable intensities confirms successful lignin extraction while maintaining aromatic methoxy groups intact. This suggests that S-rich lignin fragments remain dissolved in the ionic liquid phase during precipitation, resulting in selective recovery of G-rich pine lignin in mixed systems. Furthermore, the preservation of PCA/FA across all samples supports selective lignin precipitation and confirms that pine does not chemically inhibit *Miscanthus* fractionation.

At $R_{0\gamma} \simeq 15000$ *p*–hydroxyphenyl peaks were no longer detected. Extended treatment may additionally enable C_2/C_6 substitution, resulting in highly cross-linked, multi-substituted aromatic structures [7]. $H_{2,6}$ signals (δ_H/δ_C 7.04/127.90 ppm) present in T3 and T6 samples completely disappear in all T7 samples which is suggestive of this effect. However, it is mechanistically unclear due to the inherently low concentrations condensation products that could be volatile, like furfural, thus evaporating during freeze drying. Reports of temperature-dependent full degradation of H-units in pretreatments with deep eutectic solvents which are closely related

to ionic liquids [36, 28] do support a likelihood of this observation.
Retention of native lignin linkages provides insight into the nature of depolymerisation. β-O-4 aryl ether and ester linkages are weakly present IonoSolv causes more than 80% depolymerisation during the initial stage of the pretreatment through the cleavage of β-O-4 aryl ether linkages and ester linkages [7]. Moreover, B_γ signals from $\beta - \beta$ resinol structures (δ_H/δ_C 3.36/72.14 ppm) are maintained across samples, indicating incomplete depolymerisation despite the very high severity . Guaiacyl aromatic signals (G_2, G_5, G_6) maintain strong intensities throughout, with G_5 signals at δ_H/δ_C 6.65-6.69/114.88-115.04 ppm showing high volumes†, confirming the recalcitrance of G-type lignin structures [8].
Critically, no novel cross-peaks appear in mixed-feedstock spectra that are absent from individual feedstock controls, providing strong evidence against chemical cross-condensation between pine and *Miscanthus* lignin populations. Peak intensities in mixed samples appear as weighted contributions from individual feedstocks indicates that the two lignin populations extract and precipitate independently.

5 Future work and limitations

Analytical method refinement
The current NIR-based compositional model employs *Miscanthus* as the denominator in calculations, which may introduce systematic bias when analyzing mixed feedstock systems. Future work should develop and validate mixed-feedstock specific calibration models to improve compositional accuracy across varying biomass ratios [12]. Additionally, comprehensive statistical validation with multiple replicates ($n \geq 3$) is essential to distinguish genuine synergistic or antagonistic effects from experimental variability, as single measurements cannot definitively establish interaction mechanisms.

Process engineering optimization
The inherent challenge of achieving isothermal conditions at bench scale represents a significant limitation, as temperature gradients during pretreatment may influence extraction kinetics differently for each feedstock component [2]. Scaling to stirred tank reactor systems would enable better temperature control and mass transfer, potentially revealing interaction effects masked by current experimental limitations [19]. Furthermore, systematic investigation of the ionic liquid saturation capacity during mixed feedstock processing would establish critical feedstock ratio thresholds beyond which the more reactive *Miscanthus* component interferes with effective pine delignification.

Process innovation
The differential extraction kinetics observed between *Miscanthus* and pine lignin populations suggest potential for staged fractionation strategies. A two-stage processing approach could be beneficial: an initial lower temperature stage (150 –

$160°C$) to selectively extract intact S-rich *Miscanthus* lignin, followed by a higher severity stage targeting G-rich pine lignin extraction. This strategy could preserve valuable S-lignin structures while achieving effective pine delignification, potentially yielding two distinct lignin streams for differentiated valorization [29]. Such an approach aligns with emerging biorefinery concepts that maximize value extraction through product diversification.

Economic and sustainability assessment
Comprehensive techno-economic analysis (TEA) comparing single versus mixed feedstock processing is crucial for industrial implementation. This analysis should consider feedstock availability, seasonal variations, processing costs, and product value streams from both cellulose and differentiated lignin products [37]. Life cycle assessment would further establish the environmental benefits of mixed feedstock processing, particularly regarding reduced transportation requirements and improved biorefinery flexibility.

Broader feedstock combinations
Future investigations should extend beyond *Miscanthus*–pine systems to explore other grass-softwood combinations and potentially hardwood-softwood or grass-hardwood mixtures. Understanding how different lignin chemistries interact during IonoSolv processing would enable development of generalized processing strategies for diverse feedstock streams [28]. This knowledge would be particularly valuable for regions with varied biomass availability and for biorefineries seeking to maximize operational flexibility.

6 Conclusions

This study represents the first systematic investigation of mixed grass-softwood feedstock processing using IonoSolv pretreatment with
$[TEA][HSO_4]$. Analytical characterization using NIR-based compositional analysis and HSQC NMR spectroscopy has revealed fundamental insights into the behaviour of mixed lignin populations during ionic liquid-based fractionation.

The primary finding demonstrates that mixed *Miscanthus*-pine systems exhibit additive rather than synergistic behaviour during IonoSolv pretreatment. Glucan recovery and hemicellulose removal in mixed feedstock systems closely aligned with weighted averages of single feedstock performance, indicating independent extraction of each biomass component. However, delignification patterns revealed more complex behaviour, with 1:1 mixing ratios achieving optimal performance across all severity conditions tested. This optimization likely results from balanced ionic liquid solvating capacity that prevents saturation while maintaining efficient mass transfer. HSQC NMR analysis provided definitive evidence against chemical cross-condensation between pine and *Miscanthus* lignin populations. The complete ab-

sence of syringyl signals in mixed feedstock lignin samples, despite their clear presence in pure *Miscanthus* controls, indicates selective precipitation rather than complete degradation. The persistence of diagnostic grass markers (PCA/FA) and preservation of methoxyl signals confirms that both lignin populations extract successfully but undergo differential precipitation from the ionic liquid phase. This selective recovery mechanism, driven by the distinct solubility properties of S-rich *Miscanthus* lignin versus G-only pine lignin, represents a key mechanistic insight for mixed feedstock processing.

The sequential extraction kinetics observed, where *Miscanthus* lignin extracts rapidly during initial heating phases while pine lignin requires more severe conditions, aligns with the significant differences in glass transition temperatures between these feedstocks. This temporal separation of extraction creates opportunities for staged fractionation strategies that could enable differentiated lignin valorization pathways in integrated biorefineries [29].

From a practical biorefinery perspective, these findings demonstrate that grass-softwood co-processing is technically feasible without requiring fundamental process modifications. The absence of antagonistic effects and the predictable additive behaviour simplifies process design and optimisation for mixed feedstock operations. The ability to process diverse feedstock streams using a single pretreatment technology enhances biorefinery flexibility and economic viability.

The broad identification of a optimal processing windows ($\sim$160 $^{\circ}C$ for *Miscanthus*-rich ratios) and the understanding of differential lignin precipitation mechanisms provide actionable parameters for industrial implementation with future work should focus on statistical validation for process optimisation and exploring the valorization potential of the differentially precipitated lignin fractions. This research contributes to the broader goal of developing flexible, economically viable biorefineries capable of converting diverse lignocellulosic feedstocks into sustainable chemicals and materials, advancing the transition towards a circular bioeconomy.

7 Acknowledgements

I would like to sincerely thank and acknowledge Suhaib Nisar and Agnieszka Brandt-Talbot for their continuous support throughout the research project. Also, I would like to thank Jason Hallett and all the group members at the Hallett Group for their hospitality and welcoming me into their laboratory. I acknowledge financial support via a grant from the Laidlaw Foundation.

8 Supplementary Information (ESI)

8.1 IonoSolv protocol

IonoSolv fractionation experiments were performed according to the standard procedure highlighted previously.
For the pretreatments, the required amounts of biomass and ionic liquid were mixed thoroughly in 15 mL pressure tubes (Aceglass) and placed into a pre-heated convection oven for the required time and temperature. Tubes were left for 60 min to cool at room temperature and contents were then using absolute ethanol (40 mL) into 50 mL falcon tubes.
Pulp washing procedure was repeated 4 times where the mixture was centrifuged 4 times at 3000 $\times$ g for 20 min, with the solid and liquid phases separated by careful decanting.
Residual IL and lignin were removed from the pulp by overnight Soxhlet extraction, with the pulp-containing thimbles left to dry overnight. Ethanol was removed from the extracted IL and lignin mxiture through rotary evaporation.
Lignin was precipitated by the addition of de-ionised water (30 mL) into the re-concentrated IL. The slurry was transferred into a falcon tube then left for 30 min to ensure lignin precipitation. The slurry was washed 4 times by centrifuging at 2000 $\times$ g for 20 min, separating the solid and liquid phases by decanting. The solid lignin was then dried for 48 hr in a freeze-drier.
Moisture contents of the pulps and raw biomass were determined by weighing a portion of the samples before and after drying in a 105 $^{\circ}C$ convection oven (VWR Venti-Line 115) overnight.

8.2 NIR spectrometer settings

For all sample scans, the spectrometer-specific settings on the Agilent Cary 5000 UV-Vis-NIR spectrometer used with an internal DRA-2500 accessory were:

- Baseline correction: 100%T
- Scan range: 800-2500 nm
- Data interval: 4 nm
- Scan rate: 2400 nm min^{-1}
- NIR SBW: 2 nm
- Double beam: Normal
- Slit height: Full

8.3 HSQC Spectra

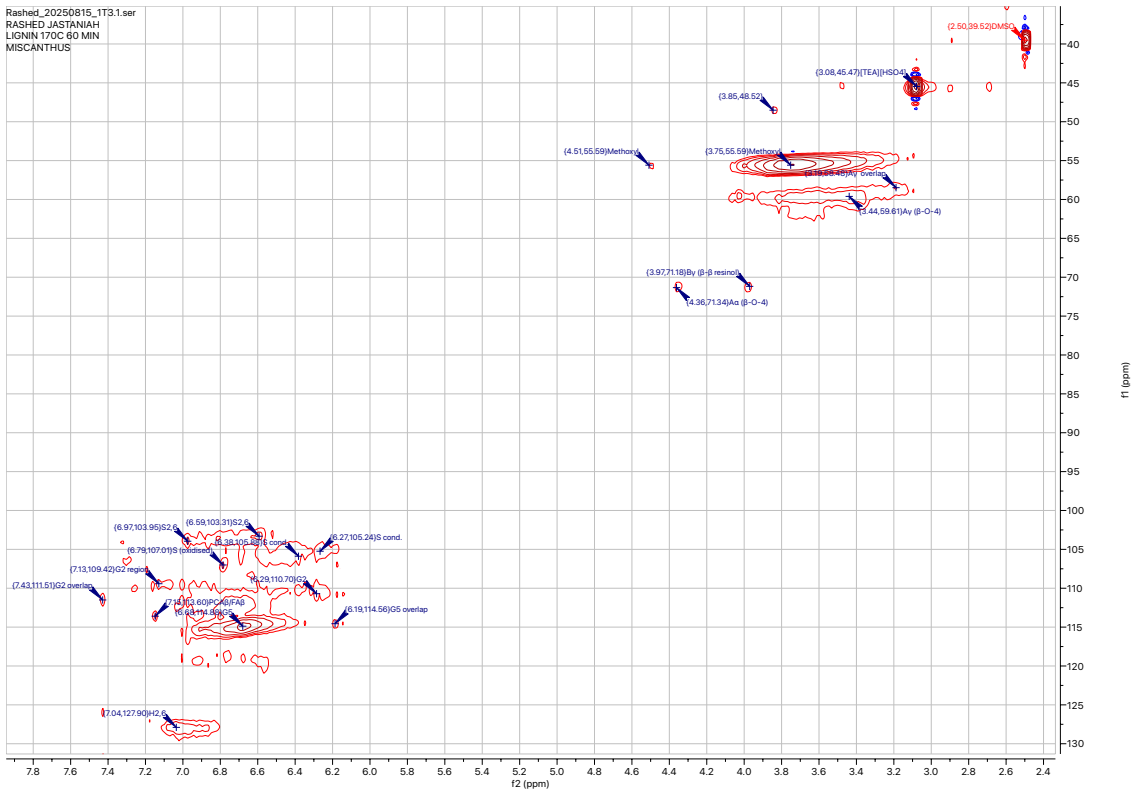

Figure 6: Annotated HSQC Spectrum of pure *Miscanthus* precipitated lignin at 170°C, 60 min and 1.005 acid-base ratio

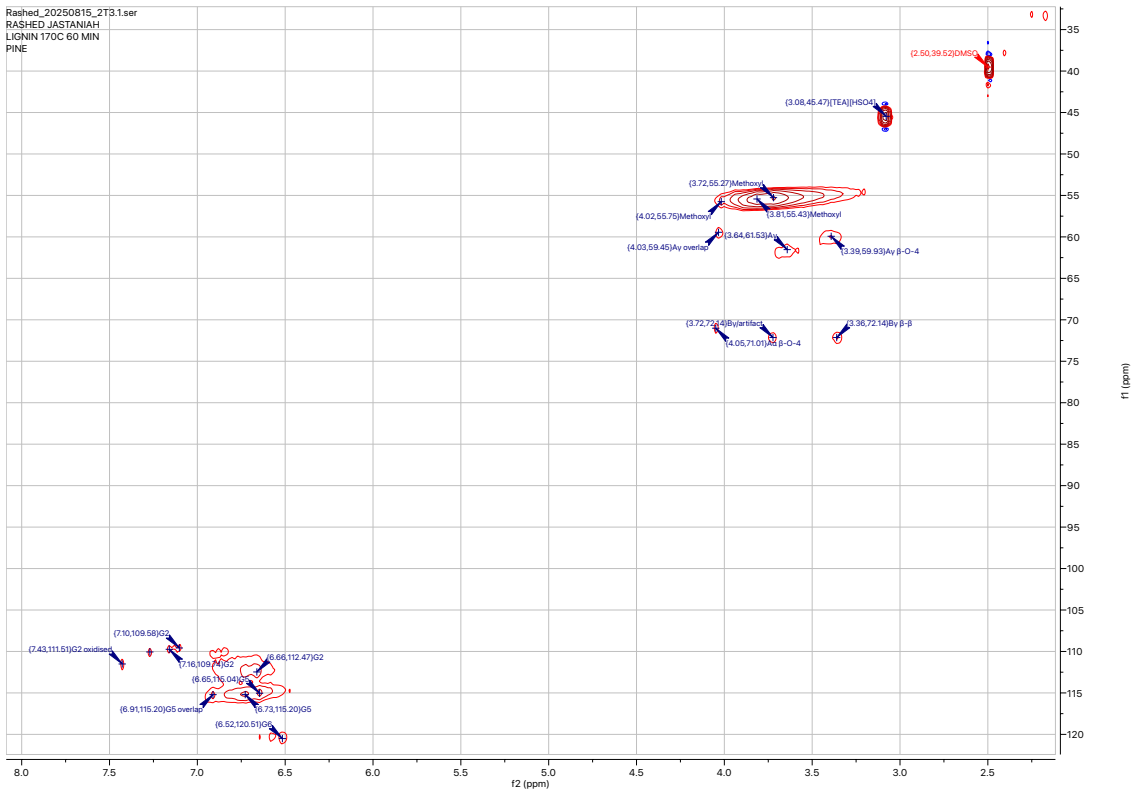

Figure 7: Annotated HSQC Spectrum of pure pine precipitated lignin at 170°C, 60 min and 1.005 acid-base ratio

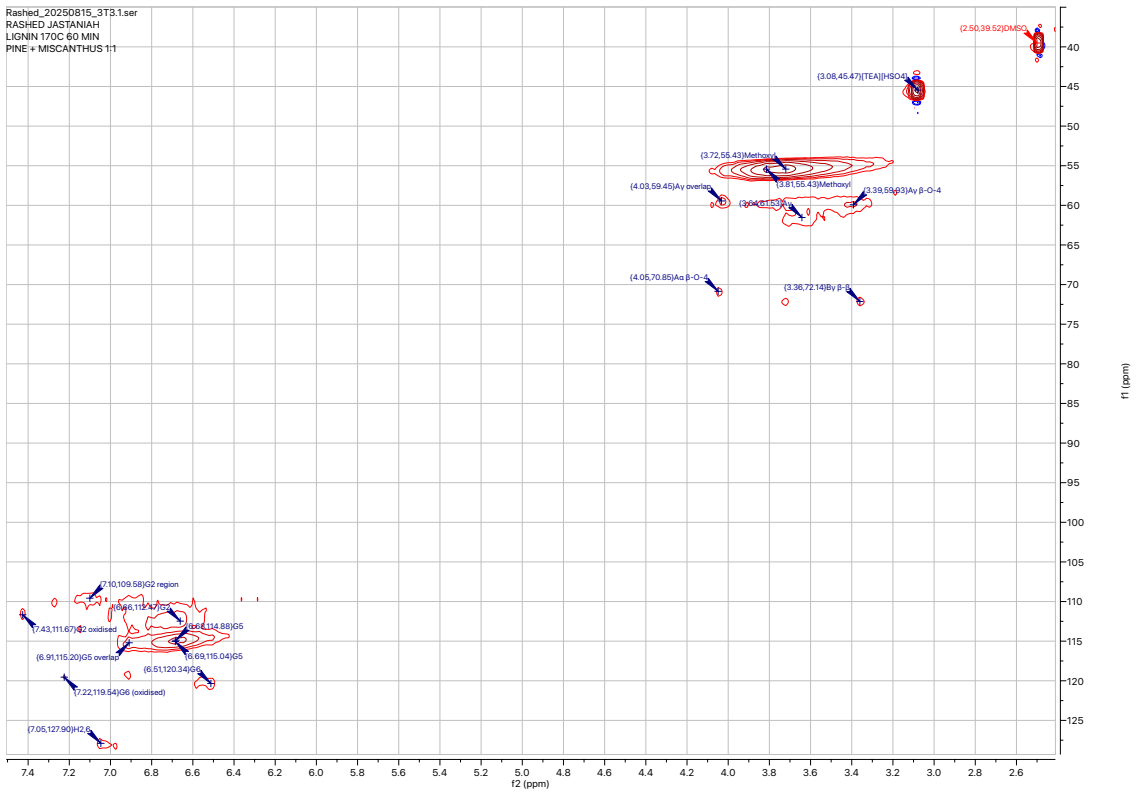

Figure 8: Annotated HSQC Spectrum of mixed (1:1 w/w) precipitated lignin at 170°C, 60 min and 1.005 acid-base ratio

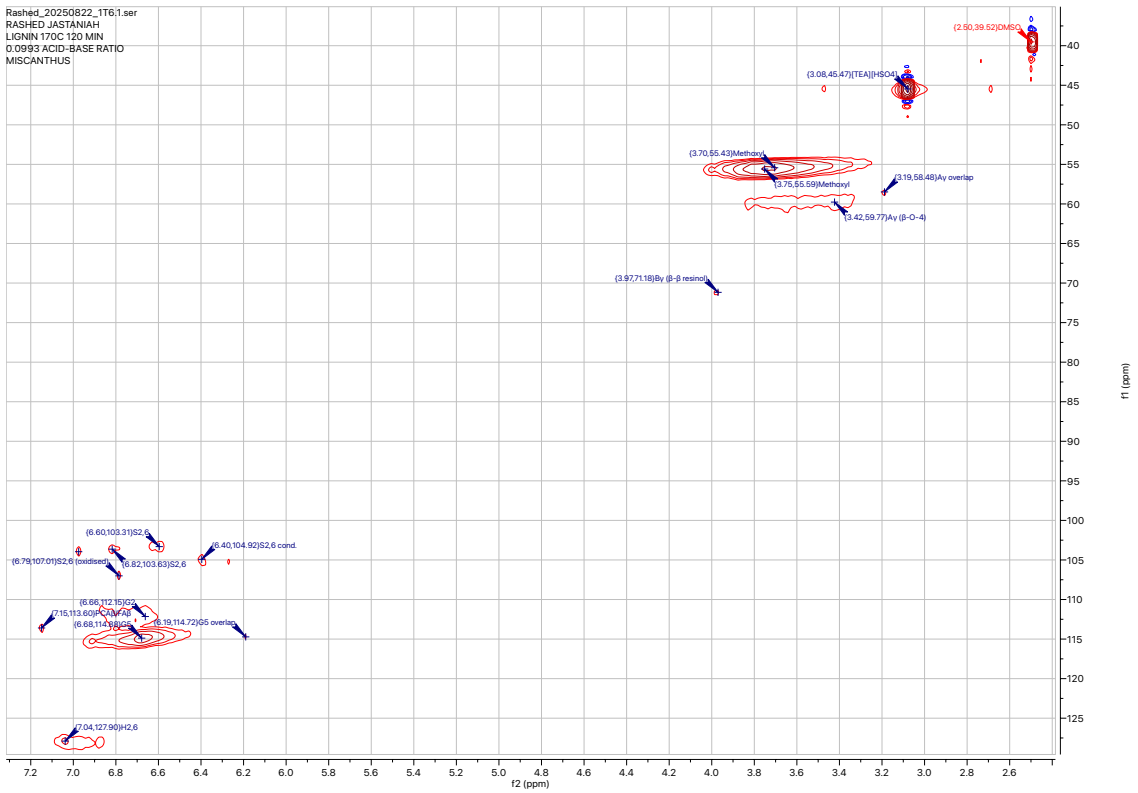

Figure 9: Annotated HSQC Spectrum of pure *Miscanthus* precipitated lignin at 170°C, 120 min and 0.993 acid-base ratio

Figure 10: Annotated HSQC Spectrum of mixed (1:1 w/w) precipitated lignin at 170°C, 120 min and 0.993 acid-base ratio

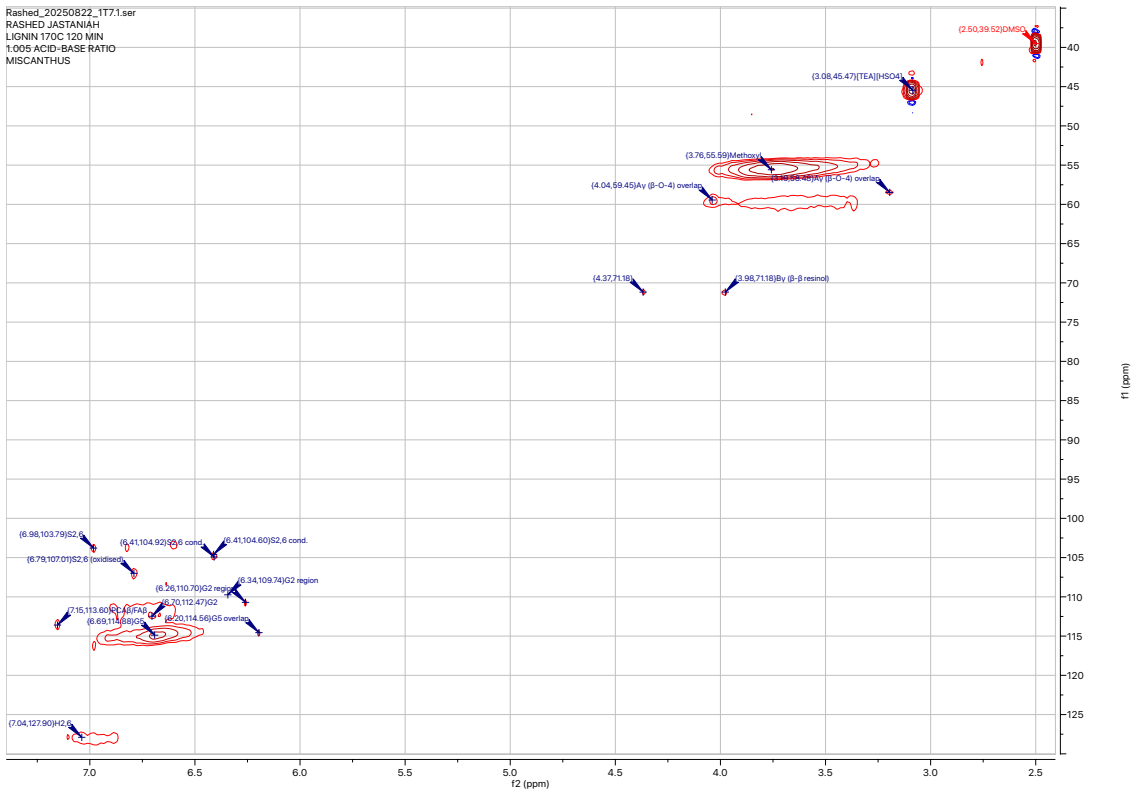

Figure 11: Annotated HSQC Spectrum of pure *Miscanthus* precipitated lignin at 170°C, 120 min and 1.005 acid-base ratio

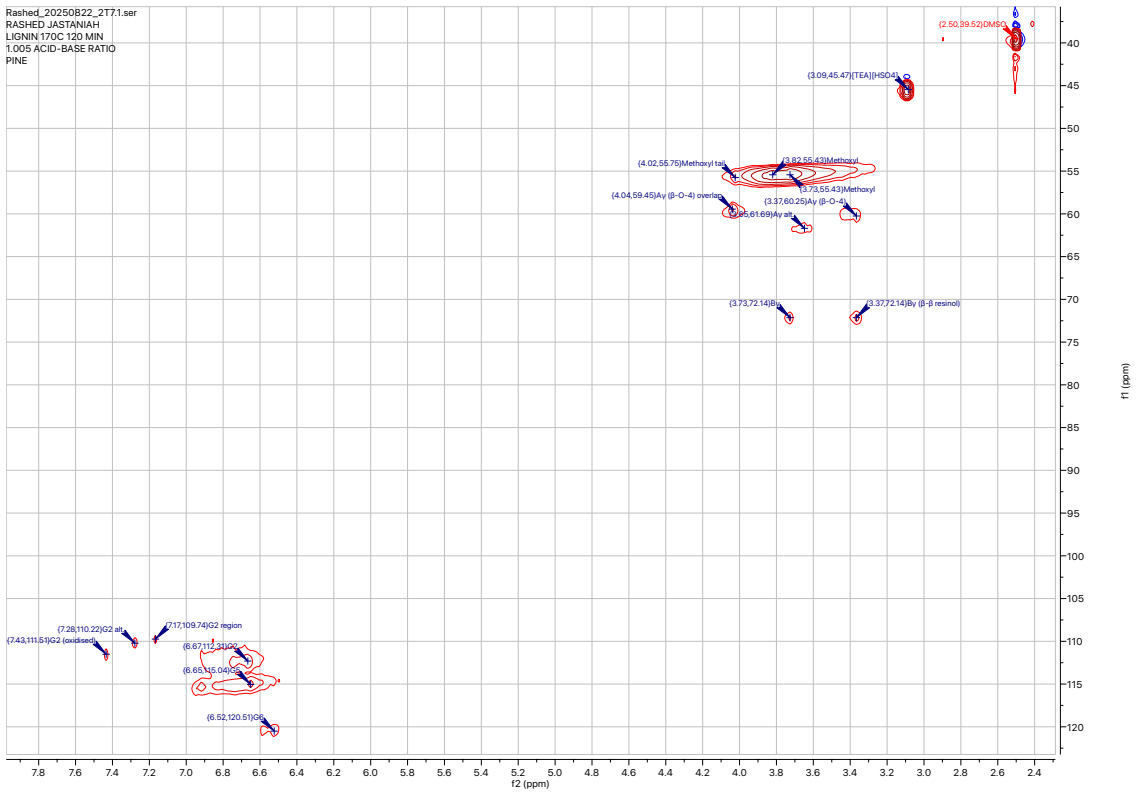

Figure 12: Annotated HSQC Spectrum of pure pine precipitated lignin at 170°C, 120 min and 1.005 acid-base ratio

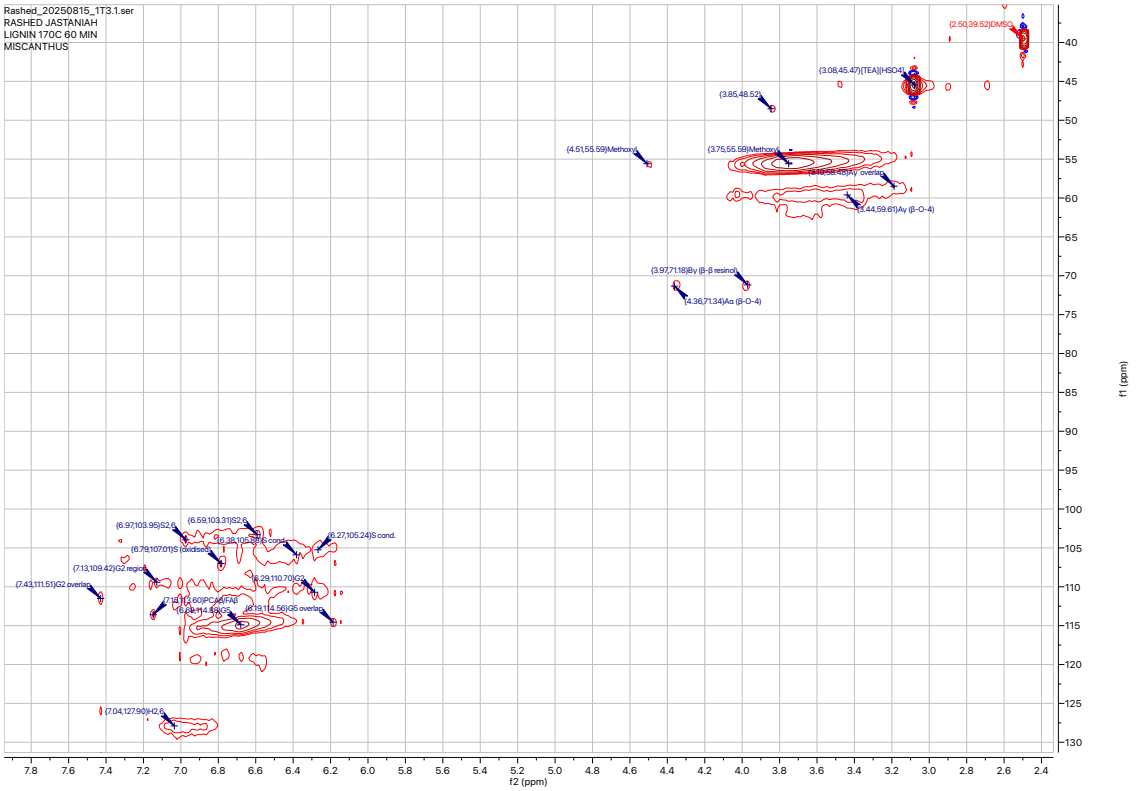

Figure 13: Annotated HSQC Spectrum of pure *Miscanthus* precipitated lignin at 170°C, 120 min and 1.005 acid-base ratio

Table 5: HSQC NMR peak assignments for lignin structural units in IonoSolv-pretreated lignocellulosic biomass. Chemical shifts represent typical ranges observed across different feedstocks (*Miscanthus giganteus*, *Pinus sylvestris*) and treatment conditions.

Label	δ_H (ppm)	δ_C (ppm)	Assignment
Aromatic region			
G2	6.29–6.70	110.70–112.47	Guaiacyl C2–H2 correlation
G2 (ox)	7.43	111.51–111.67	Oxidized guaiacyl C2–H2
G2 region	6.26–7.17	109.42–110.70	Guaiacyl C2 region (variants)
G2 (alt)	7.27–7.28	110.06–110.22	Alternative guaiacyl C2–H2
G5	6.65–6.73	114.56–115.20	Guaiacyl C5–H5 correlation
G6	6.51–6.52	120.34–120.51	Guaiacyl C6–H6 correlation
G6 (ox)	7.21–7.22	119.54	Oxidized guaiacyl C6–H6
G6 region	6.91–6.93	115.20–119.22	Guaiacyl C5/C6 overlap region
S2,6	6.59–6.98	103.31–103.95	Syringyl C2,6–H2,6 correlation
S2,6 (cond)	6.27–6.41	104.60–105.88	Condensed syringyl C2,6–H2,6
S (ox)	6.79	107.01	Oxidized syringyl units
H2,6	7.04–7.05	127.90	*p*-Hydroxyphenyl C2,6–H2,6
PCA_β/FA_β	7.15	113.60	*p*-Coumaric/ferulic acid C_β–H_β
Side chain region			
$–OCH_3$	3.70–3.82	55.27–55.75	Aromatic methoxyl groups
A_α	4.05–4.36	70.85–71.34	β-O-4 C_α–H_α
A_γ	3.39–3.44	59.61–59.93	β-O-4 C_γ–H_γ
A_γ (overlap)	3.19–4.04	58.48–59.45	β-O-4 C_γ overlap region
A_γ (alt)	3.64–3.69	61.53–62.02	Alternative β-O-4 C_γ–H_γ
B_γ	3.36–3.98	71.18–72.14	Resinol (β–β) C_γ–H_γ
Reference signals			
[TEA][HSO_4]	3.08–3.09	45.47	Triethylammonium hydrogensulphate Ionic liquid
DMSO-d_6	2.50	39.52	NMR solvent

8.4 $R_{0\gamma}$ coefficient optimisation

The modified severity factor was defined by adding an exponential term dependent on the acid-base ratio:

$$R_{0\gamma} = \left(t \cdot e^{\frac{T-T_{ref}}{\omega}} \right) \cdot e^{\gamma(R-1)} = R_0 \cdot e^{\gamma(R-1)}$$

In logarithmic form, this equation becomes a linear relationship:

$$\log(R_{0\gamma}) = \log(R_0) + \gamma(R-1)$$

The coefficient γ represents the weighting of the acid-base ratio's contribution to overall severity. This coefficient was empirically optimized using the dataset from this study (35 samples across 7 distinct conditions).

The value of γ was determined by performing correlation analysis between the calculated $\log(R_{0\gamma})$ and the key experimental performance metrics: Glucan Recovery, Hemicellulose Removal, and Delignification. The value of $\gamma = 20$ was selected as it provided the maximum coefficient of determination (R^2) across all metrics, significantly improving the predictive power of the severity factor compared to the classical $R_{0\gamma}$.

Validation of the Optimized Coefficient

Including the acid-base ratio term with $\gamma = 20$ substantially improved the correlation between the calculated severity and the observed experimental results. As shown in Table 6, the R^2 values for key metrics improved by 4-39%, with all correlations being highly significant ($p < 0.0001$). This confirms that the acid-base ratio has a moderate but statistically significant effect on the fractionation process.

Table 6: Improvement in coefficient of determination (R^2) after incorporating the acid-base ratio term ($\gamma = 20$) into the severity factor.

Performance Metric	R^2 **(Classical** R_0**)**	R^2 **(Modified** $R_{0\gamma}$**)**	**Improvement**
Glucan Recovery	0.446	0.620	+39%
Delignification	0.534	0.623	+17%
Hemicellulose Removal	0.426	0.445	+4%

Final Severity Factor Values The calculated severity factors for the 7 conditions investigated in this study are provided in Table 7.

Table 7: Calculated Severity Factor (SF) and Normalized Severity Factor (SF_{scaled}) for the 7 experimental conditions, using $\gamma = 20$.

Temperature (°C)	Duration (min)	Acid-Base Ratio	$R_{0\gamma}$	$R_{0\gamma,\textbf{scaled}}$
150	90	0.993	1934	0.000
160	60	0.993	2540	0.039
160	60	1.005	4413	0.160
170	60	0.993	5003	0.199
170	60	1.005	8694	0.437
170	120	0.993	10006	0.522
170	120	1.005	17388	1.000

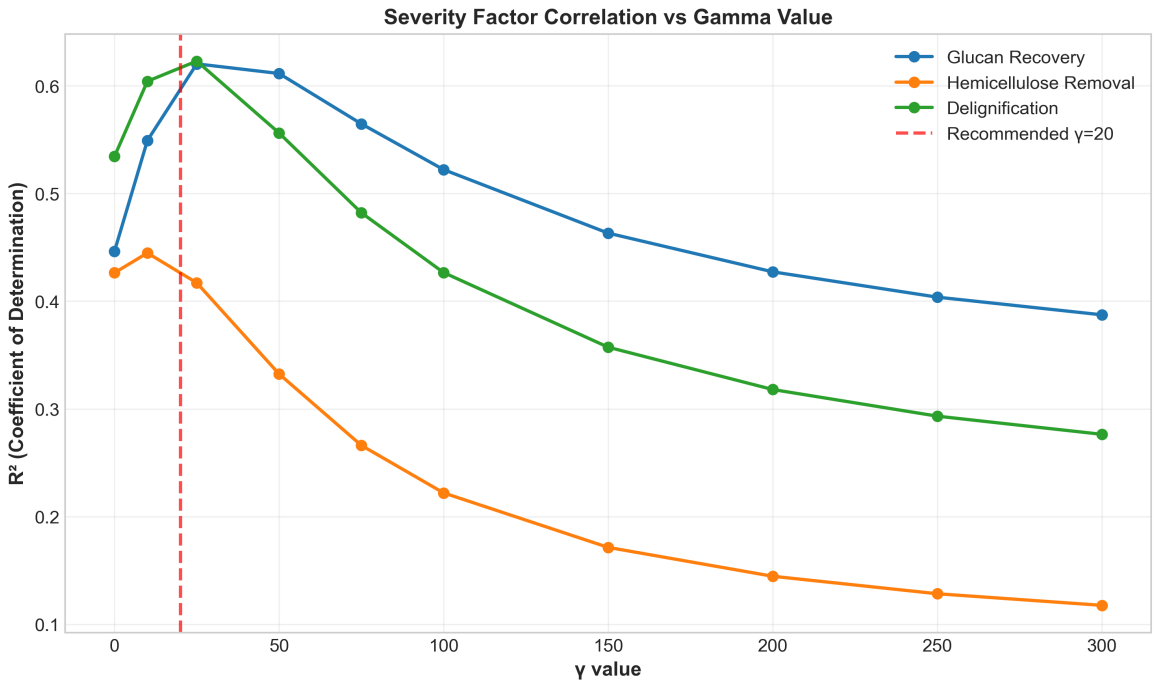

Figure 14: R^2 vs γ value

References

[1] Magda Titirici et al. “The sustainable materials roadmap”. en. In: **Journal of Physics: Materials** 5.3 (Aug. 2022). Publisher: IOP Publishing, p. 032001. ISSN: 2515-7639. DOI: 10.1088/2515-7639/ac4ee5. URL: https://doi.org/10.1088/2515-7639/ac4ee5 (visited on 11/12/2025).

[2] Agnieszka Brandt-Talbot et al. “An economically viable ionic liquid for the fractionation of lignocellulosic biomass”. en. In: **Green Chemistry** 19.13 (2017), pp. 3078–3102. ISSN: 1463-9262, 1463-9270. DOI: 10.1039/C7GC00705A. URL: https://xlink.rsc.org/?DOI=C7GC00705A (visited on 10/31/2025).

[3] Agnieszka Brandt et al. “Deconstruction of lignocellulosic biomass with ionic liquids”. en. In: **Green Chemistry** 15.3 (2013), p. 550. ISSN: 1463-9262,

1463-9270. DOI: 10.1039/c2gc36364j. URL: https://xlink.rsc.org/?DOI=c2gc36364j (visited on 10/31/2025).

[4] Anthe George et al. "Design of low-cost ionic liquids for lignocellulosic biomass pretreatment". en. In: **Green Chemistry** 17.3 (2015), pp. 1728–1734. ISSN: 1463-9262, 1463-9270. DOI: 10.1039/C4GC01208A. URL: https://xlink.rsc.org/?DOI=C4GC01208A (visited on 10/31/2025).

[5] Florence J. V. Gschwend et al. "Pretreatment of Lignocellulosic Biomass with Low-cost Ionic Liquids". en. In: **Journal of Visualized Experiments (JoVE)** 114 (Aug. 2016), e54246. ISSN: 1940-087X. DOI: 10.3791/54246. URL: https://app.jove.com/t/54246/pretreatment-of-lignocellulosic-biomass-with-low-cost-ionic-liquids (visited on 10/31/2025).

[6] Florence J. V. Gschwend et al. "Rapid pretreatment of *Miscanthus* using the low-cost ionic liquid triethylammonium hydrogen sulfate at elevated temperatures". en. In: **Green Chemistry** 20.15 (2018), pp. 3486–3498. ISSN: 1463-9262, 1463-9270. DOI: 10.1039/C8GC00837J. URL: https://xlink.rsc.org/?DOI=C8GC00837J (visited on 10/31/2025).

[7] Agnieszka Brandt et al. "Structural changes in lignins isolated using an acidic ionic liquid water mixture". en. In: **Green Chemistry** 17.11 (2015), pp. 5019–5034. ISSN: 1463-9262, 1463-9270. DOI: 10.1039/C5GC01314C. URL: https://xlink.rsc.org/?DOI=C5GC01314C (visited on 10/31/2025).

[8] Florence J. V. Gschwend et al. "Quantitative glucose release from softwood after pretreatment with low-cost ionic liquids". en. In: **Green Chemistry** 21.3 (2019), pp. 692–703. ISSN: 1463-9262, 1463-9270. DOI: 10.1039/C8GC02155D. URL: https://xlink.rsc.org/?DOI=C8GC02155D (visited on 10/31/2025).

[9] Klaus A. Y. Koivu et al. "Effect of Fatty Acid Esterification on the Thermal Properties of Softwood Kraft Lignin". en. In: **ACS Sustainable Chemistry & Engineering** 4.10 (Oct. 2016), pp. 5238–5247. ISSN: 2168-0485, 2168-0485. DOI: 10.1021/acssuschemeng.6b01048. URL: https://pubs.acs.org/doi/10.1021/acssuschemeng.6b01048 (visited on 11/03/2025).

[10] A Sluiter. "Determination of Total Solids in Biomass and Total Dissolved Solids in Liquid Process Samples: Laboratory Analytical Procedure (LAP)". en. In: **Technical Report** (2008).

[11] Aida R. Abouelela et al. "Evaluating the Role of Water as a Cosolvent and an Antisolvent in [HSO_4]-Based Protic Ionic Liquid Pretreatment". en. In: **ACS Sustainable Chemistry & Engineering** 9.31 (Aug. 2021), pp. 10524–10536. ISSN: 2168-0485, 2168-0485. DOI: 10.1021/acssuschemeng.1c02299. URL: https://pubs.acs.org/doi/10.1021/acssuschemeng.1c02299 (visited on 10/31/2025).

[12] Suhaib Nisar et al. "Near-infrared spectroscopy for rapid compositional analysis of cellulose pulps after fractionation with ionic liquids". In: **Biomass and Bioenergy** 201 (Oct. 2025), p. 108056. ISSN: 0961-9534. DOI: 10.1016/j.biombioe.2025.108056. URL: https://www.sciencedirect.com/science/article/pii/S0961953425004672 (visited on 10/31/2025).

[13] R. P. Overend and E. Chornet. “Fractionation of lignocellulosics by steam-aqueous pretreatments”. In: **Philosophical Transactions of the Royal Society of London. Series A, Mathematical and Physical Sciences** 321.1561 (Apr. 1987). Publisher: Royal Society, pp. 523–536. DOI: 10.1098/rsta.1987.0029. URL: https://royalsocietypublishing.org/doi/10.1098/rsta.1987.0029 (visited on 11/05/2025).

[14] Francisco Malaret et al. “*Eucalyptus red grandis* pretreatment with protic ionic liquids: effect of severity and influence of sub/super-critical CO_2 atmosphere on pretreatment performance”. en. In: **RSC Advances** 10.27 (2020), pp. 16050–16060. ISSN: 2046-2069. DOI: 10.1039/D0RA02040K. URL: https://xlink.rsc.org/?DOI=D0RA02040K (visited on 10/31/2025).

[15] D. Montané et al. “Phenomenological kinetics of wood delignification: application of a time-dependent rate constant and a generalized severity parameter to pulping and correlation of pulp properties”. en. In: **Wood Science and Technology** 28.6 (Sept. 1994), pp. 387–402. ISSN: 1432-5225. DOI: 10.1007/BF00225458. URL: https://doi.org/10.1007/BF00225458 (visited on 11/05/2025).

[16] Aida R. Abouelela, Pedro Y. S. Nakasu, and Jason P. Hallett. “Influence of Pretreatment Severity Factor and Hammett Acidity on Softwood Fractionation by an Acidic Protic Ionic Liquid”. en. In: **ACS Sustainable Chemistry & Engineering** 11.6 (Feb. 2023), pp. 2404–2415. ISSN: 2168-0485, 2168-0485. DOI: 10.1021/acssuschemeng.2c06076. URL: https://pubs.acs.org/doi/10.1021/acssuschemeng.2c06076 (visited on 10/31/2025).

[17] Pedro Y.S. Nakasu et al. “Pretreatment of biomass with protic ionic liquids”. en. In: **Trends in Chemistry** 4.3 (Mar. 2022), pp. 175–178. ISSN: 25895974. DOI: 10.1016/j.trechm.2021.12.001. URL: https://linkinghub.elsevier.com/retrieve/pii/S258959742100277X (visited on 10/31/2025).

[18] Wei-Chien Tu et al. “Characterisation of cellulose pulps isolated from Miscanthus using a low-cost acidic ionic liquid”. en. In: **Cellulose** 27.8 (May 2020), pp. 4745–4761. ISSN: 0969-0239, 1572-882X. DOI: 10.1007/s10570-020-03073-1. URL: http://link.springer.com/10.1007/s10570-020-03073-1 (visited on 10/31/2025).

[19] Clementine L. Chambon et al. “Process intensification of the ionoSolv pretreatment: effects of biomass loading, particle size and scale-up from 10 mL to 1 L”. en. In: **Scientific Reports** 11.1 (July 2021), p. 15383. ISSN: 2045-2322. DOI: 10.1038/s41598-021-94629-z. URL: https://www.nature.com/articles/s41598-021-94629-z (visited on 10/31/2025).

[20] Atanu Kumar Das et al. “Multi-blade milling from log to powder in one step – Experimental design and results”. In: **Powder Technology** 378 (Jan. 2021), pp. 593–601. ISSN: 0032-5910. DOI: 10.1016/j.powtec.2020.10.026. URL: https://www.sciencedirect.com/science/article/pii/S0032591020309694 (visited on 11/07/2025).

[21] Z. Miao et al. “Energy requirement for comminution of biomass in relation to particle physical properties”. In: **Industrial Crops and Products** 33.2 (Mar. 2011), pp. 504–513. ISSN: 0926-6690. DOI: 10.1016/j.indcrop.2010.12.016. URL: https://www.sciencedirect.com/science/article/pii/S0926669010003365 (visited on 11/07/2025).

[22] Agi Brandt-Talbot et al. **Treatment of biomass to dissolve lignin with ionic liquid composition**. US Patent US9765478B2. Sept. 2017. URL: https://patents.google.com/patent/US9765478B2.

[23] T. E. Timell. “Recent progress in the chemistry of wood hemicelluloses”. en. In: **Wood Science and Technology** 1.1 (1967), pp. 45–70. ISSN: 0043-7719, 1432-5225. DOI: 10.1007/BF00592255. URL: http://link.springer.com/10.1007/BF00592255 (visited on 11/03/2025).

[24] Weiying Li et al. “Rapid dissolution of lignocellulosic biomass in ionic liquids using temperatures above the glass transition of lignin”. en. In: **Green Chemistry** 13.8 (2011), p. 2038. ISSN: 1463-9262, 1463-9270. DOI: 10.1039/c1gc15522a. URL: https://xlink.rsc.org/?DOI=c1gc15522a (visited on 11/03/2025).

[25] Oleg V. Startsev et al. “Impact of moisture content on dynamic mechanical properties and transition temperatures of wood”. In: **Wood Material Science & Engineering** 12.1 (Jan. 2017). Publisher: Taylor & Francis _eprint: https://doi.org/10.1080/17480272.2015.1020566, pp. 55–62. ISSN: 1748-0272. DOI: 10.1080/17480272.2015.1020566. URL: https://doi.org/10.1080/17480272.2015.1020566 (visited on 11/10/2025).

[26] Shawn D. Mansfield et al. “Whole plant cell wall characterization using solution-state 2D NMR”. en. In: **Nature Protocols** 7.9 (Sept. 2012). Publisher: Nature Publishing Group, pp. 1579–1589. ISSN: 1750-2799. DOI: 10.1038/nprot.2012.064. URL: https://www.nature.com/articles/nprot.2012.064 (visited on 11/10/2025).

[27] Ewellyn A. Capanema et al. “Structural Analysis of Residual and Technical Lignins by 1H-13C Correlation 2D NMR-Spectroscopy”. en. In: 55.3 (Apr. 2001). Publisher: De Gruyter Section: Holzforschung, pp. 302–308. ISSN: 1437-434X. DOI: 10.1515/HF.2001.050. URL: https://www.degruyterbrill.com/document/doi/10.1515/HF.2001.050/html?utm_source=researchgate.net&medium=article (visited on 11/10/2025).

[28] Tanmoy Dutta et al. “Characterization of Lignin Streams during Bionic Liquid-Based Pretreatment from Grass, Hardwood, and Softwood”. In: **ACS Sustainable Chemistry & Engineering** 6.3 (Mar. 2018). Publisher: American Chemical Society, pp. 3079–3090. DOI: 10.1021/acssuschemeng.7b02991. URL: https://doi.org/10.1021/acssuschemeng.7b02991 (visited on 11/10/2025).

[29] Meng Chen et al. “Design of a combined ionosolv-organosolv biomass fractionation process for biofuel production and high value-added lignin valorisation”. en. In: **Green Chemistry** 22.15 (2020), pp. 5161–5178. ISSN: 1463-9262, 1463-9270. DOI: 10.1039/D0GC01143F. URL: https://xlink.rsc.org/?DOI=D0GC01143F (visited on 10/31/2025).

[30] José C. del Río et al. “Structural Characterization of Wheat Straw Lignin as Revealed by Analytical Pyrolysis, 2D-NMR, and Reductive Cleavage Methods”. In: **Journal of Agricultural and Food Chemistry** 60.23 (June 2012). Publisher: American Chemical Society, pp. 5922–5935. ISSN: 0021-8561. DOI: 10.1021/jf301002n. URL: https://doi.org/10.1021/jf301002n (visited on 11/10/2025).

[31] Ralph, Sally A., Ralph, John, and Lu, Fachuang. **NMR Database of Lignin and Cell Wall Model Compounds**. 2024. DOI: https://doi.org/10.11578/2409191.

[32] Ewellyn A. Capanema, Mikhail Yu. Balakshin, and John F. Kadla. “Quantitative Characterization of a Hardwood Milled Wood Lignin by Nuclear Magnetic Resonance Spectroscopy”. In: **Journal of Agricultural and Food Chemistry** 53.25 (Dec. 2005). Publisher: American Chemical Society, pp. 9639–9649. ISSN: 0021-8561. DOI: 10.1021/jf0515330. URL: https://doi.org/10.1021/jf0515330 (visited on 11/10/2025).

[33] Ting-Ting You et al. “Structural Elucidation of the Lignins from Stems and Foliage of Arundo donax Linn.” In: **Journal of Agricultural and Food Chemistry** 61.22 (June 2013). Publisher: American Chemical Society, pp. 5361–5370. ISSN: 0021-8561. DOI: 10.1021/jf401277v. URL: https://doi.org/10.1021/jf401277v (visited on 11/10/2025).

[34] Kun Cheng et al. “Solution-State 2D NMR Spectroscopy of Plant Cell Walls Enabled by a Dimethylsulfoxide-d6/1-Ethyl-3-methylimidazolium Acetate Solvent”. In: **Analytical Chemistry** 85.6 (Mar. 2013). Publisher: American Chemical Society, pp. 3213–3221. ISSN: 0003-2700. DOI: 10.1021/ac303529v. URL: https://doi.org/10.1021/ac303529v (visited on 11/10/2025).

[35] Roland El Hage et al. “Characterization of milled wood lignin and ethanol organosolv lignin from *miscanthus*”. In: **Polymer Degradation and Stability** 94.10 (Oct. 2009), pp. 1632–1638. ISSN: 0141-3910. DOI: 10.1016/j.polymdegradstab.2009.07.007. URL: https://www.sciencedirect.com/science/article/pii/S0141391009002432 (visited on 11/10/2025).

[36] Qinghua Ji et al. “Pretreatment of sugarcane bagasse with deep eutectic solvents affect the structure and morphology of lignin”. In: **Industrial Crops and Products** 173 (Dec. 2021), p. 114108. ISSN: 0926-6690. DOI: 10.1016/j.indcrop.2021.114108. URL: https://www.sciencedirect.com/science/article/pii/S0926669021008736 (visited on 11/10/2025).

[37] Husain Baaqel et al. “Role of life-cycle externalities in the valuation of protic ionic liquids – a case study in biomass pretreatment solvents”. en. In: **Green Chemistry** 22.10 (2020), pp. 3132–3140. ISSN: 1463-9262, 1463-9270. DOI: 10.1039/D0GC00058B. URL: https://xlink.rsc.org/?DOI=D0GC00058B (visited on 10/31/2025).